

Further Development of a Micro Hall Thruster

Tsuyohito Ito^{*}, Nicolas Gascon[†], W. Scott Crawford[‡], and Mark A. Cappelli[§]
Stanford University, Stanford, California 94305-3032

The operation and performance characterization of a micro Hall thruster is presented. The thruster is co-axial in design, with a 0.5 mm channel width and 4 mm outer diameter. The magnetic circuit includes a SmCo permanent magnet generating approximately 0.7 T at the exit plane and 1 T in the channel. Operation with a hollow cathode neutralizer is achieved in the 10-40 W power range with an anode flow rate of 0.12-0.20 mg/s Xe. The thrust is measured to be in the range of 0.6-1.6 mN for an anode flow rate of 0.17-0.20 mg/s and an applied voltage of 110-275V. Thrust efficiency and the specific impulse are in the range of 10-15 % and 300-850 s, respectively, for the same conditions. Relatively broad ion energy distributions and large beam divergence are observed from an analysis of the plume using a retarding potential analyzer and ion current probe. The thruster exhibits the characteristic “breathing mode” instability in the 35-70 kHz frequency range.

I. Introduction

THERE is increased interest in scaling Hall plasma thrusters, which have been studied since the early 1960's [1,2] down into the 10-100 W range for use on power-limited and smaller satellites. The reduction in power is concomitant with a reduction in thruster size [3,4]. The design of a low power Hall thruster should preserve the ratio of the Larmor radius to channel width (which is typically ~ 1 cm in 1 kW designs), necessitating operation at higher magnetic fields. The reduced Larmor scale increases the cyclotron frequency, allowing operation at higher gas density to preserve the classical Hall Parameter.

We have developed a prototype micro Hall thruster and operated it with a hot filament cathode [5]. The channel of this prototype thruster has an outer and inner diameter of 4 mm and 3 mm, respectively. The magnetic flux is approximately 1 T in the channel and 0.7 T at the exit plane. The thruster was operated with a power in the range of 15-40W at a relatively high mass flow rate (0.3-0.5 mg/s Xe). The study also indicated that the cathode has a strong effect on thruster operation. Here, we characterize the operation of this micro Hall thruster with a hollow cathode neutralizer. The thruster is operated with 10-40W of discharge power at an anode flow rate of 0.12-0.20 mg/s Xe. We investigate the thruster plume with an ion probe (ion current density), a retarding potential analyzer (ion energy distribution function), an emissive probe (plasma potential), and we directly measure thrust to estimate the specific impulse and efficiency.

II. Experiments

A. Test facility

The plume characterization was carried out in a test facility consisting of a non-magnetic stainless steel chamber approximately 0.6 m in diameter and 1.2 m in length. The chamber is pumped by a single 50 cm diameter cryopump (CVI-TM500) backed by a ~60 l/s mechanical pump. The base pressure of the facility is approximately 10^{-4} Pa, as measured by an ionization gauge, uncorrected for xenon. Thruster testing at xenon flow rates of 0.12-0.20 mg/s results in chamber background pressure of approximately 10^{-3} Pa. Thrust measurements were carried out in a larger test facility consisting of a non-magnetic stainless steel chamber approximately 1.5 m in diameter and 3.3 m in length, and a two-stage cryogenic pumping system (CVI-TM1200). The pressure during the thrust measurements was approximately 5×10^{-4} Pa. Research grade (99.995 %) xenon is used for the main thruster discharge and for the

^{*} Postdoctoral Scholar, Mechanical Engineering Department, Building 520. Member, AIAA.

[†] Research Associate, Mechanical Engineering Department, Building 520. Member, AIAA.

[‡] Research Assistant, Mechanical Engineering Department, Building 520.

[§] Professor, Mechanical Engineering Department, Building 520. Member, AIAA.

hollow cathode, with mass flow controller accurate within 1% of the total flow rate (1.25-2 sccm, or 0.12-0.2 mg/s Xe).

B. Micro Hall Thruster

A schematic illustration of the micro Hall thruster is shown in Fig. 1. A photograph of the actual thruster is shown in Fig. 2. The magnetic circuit incorporates a ring-shaped SmCo permanent magnet in conjunction with a high purity iron circuit. The outer diameter of the magnet is 14 mm, the inner diameter is 4 mm, and the thickness is 3 mm. The outer diameter of the iron core is 3 mm, resulting in an annular channel of width $w = 0.5$ mm. The metal channel depth at anode potential is 3 mm. The insulator outer wall depth, which is the thickness of the alumina insulator covering the magnet, is approximately 230 μm , i.e., about half of the channel width. The magnetic field generated by this structure is predominately radial near the exit of the channel, as verified by simulations for this circuit carried out using a two-dimensional (2D) axisymmetric finite element solver [6]. The magnetic field strength near the exit of the channel (surface of the alumina insulator) is ~ 0.7 T and the maximum strength in the channel is approximately 1 T. For thermal management, the iron base is water-cooled, and the central pole piece is covered with a 3 mm diameter, 400 μm thick (approximately the channel width) polycrystalline diamond plate, which also serves as the channel inner wall.

The thruster main discharge is powered by a Sorensen SCR600-1.7 power supply. Anode current oscillations are monitored by measuring the voltage across a 4 Ω shunt resistor in series with the discharge. The ion plume was neutralized with a commercial hollow cathode (Ion Tech Inc., HCN-252) operating with a flow of 0.16 mg/s of xenon and located 1 cm downstream and 4 cm off the axis of the channel.

C. Performance Characterization

The plume was characterized by measuring the spatial distribution of ion current and ion energy distribution. Performance was evaluated through direct (and indirect) thrust measurements.

A guarded planar ion probe (3 mm in diameter) biased to ~ -30 V to repel the electrons was used to measure the ion current distribution and total ion current in the plume. The ion current measurements were performed 22 cm downstream of the channel exit.

The ion energy distribution was characterized by a miniaturized retarding potential analyzer (RPA), with a 4 mm entrance aperture. For the RPA measurements, the outermost grid is electrically floating, the second (electron repelling) grid is set to a potential of -25 V, and the ion retarding grid is swept to a potential of up to $+350$ V. The collector is coated with a graphite emulsion, to reduce secondary electron emission. The transmitted ion current incident onto the collector was recorded with a picoammeter (Keithley 485). More details of the RPA were presented in Ref. [5]. For the ion energy measurements, the entrance of the RPA was located 7 cm downstream of the channel exit. Plasma potential measurements required for the analysis of the RPA data were measured by emissive probe

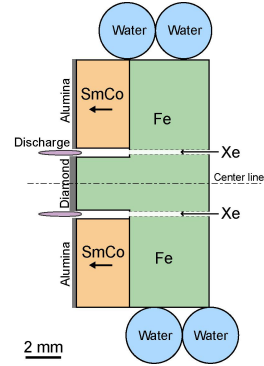


Figure 1. Schematic of micro Hall thruster.

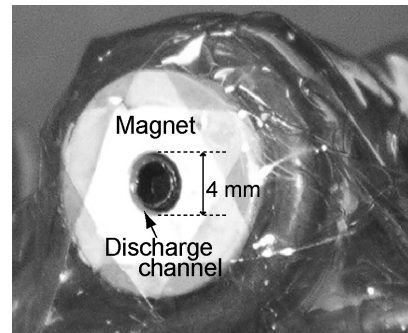


Figure 2. Photograph of micro Hall thruster.

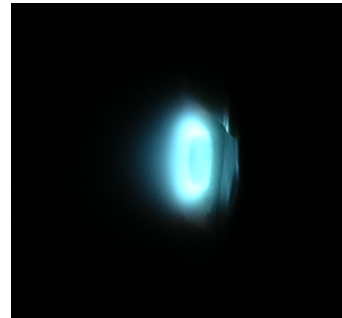


Figure 3. Photograph of micro Hall thruster during operation.

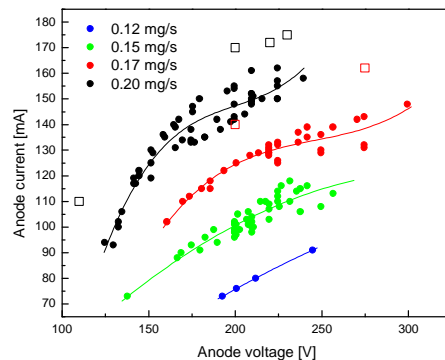


Figure 4. Voltage-Current characteristics. Note: open squares are for values observed during direct thrust measurements.

measurements at the same location. The emissive probe is a 150 μm diameter heated tungsten wire coil (5 turns). The ion probe, RPA, and emissive probe were mounted on a stepper motor-controlled rotational stage for angle-resolved measurements.

Thrust was measured with an inverted pendulum type thrust stand. The stand includes an electromechanic damper for filtering the oscillations induced by the vacuum pumping system, and is water-cooled to minimize thermal drift during thruster operation. Calibration can be performed in situ at regular intervals using an electric motor, pulleys and several weights of known masses (within 10^{-4} relative uncertainty). The thrust stand signal is linear within 1% tolerance and capable of detecting horizontal forces down to ~ 0.1 mN.

III. Results and Discussion

A. Micro Hall Thruster Operation

Figure 3 shows a photograph of the micro Hall thruster during operation. The discharge generated intense blue emission (due to excited xenon ions) in the annular channel. In all the measurements presented here, the discharge was operated in voltage limited mode. The light emission from the discharge appeared to be fairly uniform around the coaxial channel. The V - I characteristics, which are illustrated in Fig. 4, are somewhat typical of Hall discharges, although the discharge current does not saturate at high voltages, contrary to what is observed in most modern Hall thrusters. Discharge instabilities precluded operation below about 0.11 mg/s of anode flow. The discharge stability at slightly higher flow rates (0.12-0.15 mg/s) was influenced by an observed (slow) thermal drift, and although the discharge is sufficiently stable for documenting V - I curves, the operating regime was found to drift for longer running times (~ 20 min).

Figure 5 shows oscillograms of discharge current. For all the operating conditions investigated here, the discharge current exhibited strong oscillations associated with the so-called “breathing mode” instability [7]. Figure 6 depicts a spectral analysis of these oscillograms. The distributions are characterized by sharp fundamental modes in the 35-70 kHz range, with less intense harmonics, as also observed in the previous study with a wire filament neutralizer [5]. In a typical kW-level thruster, this instability is observed at 10-20 kHz. From the $\sim 1/20^{\text{th}}$ size scaling of this thruster, the breathing mode was expected to be somewhat higher in frequency. We suspect that the low frequency is due to a relatively thick ionization layer. The frequency of the fundamental component is found to vary nearly linearly with discharge voltage, as illustrated in Fig. 7.

B. Ion Current Measurement

The results of plume ion current measurements are shown in Fig. 8. The distributions are nearly symmetrical, perhaps slightly affected by the cathode neutralizer which

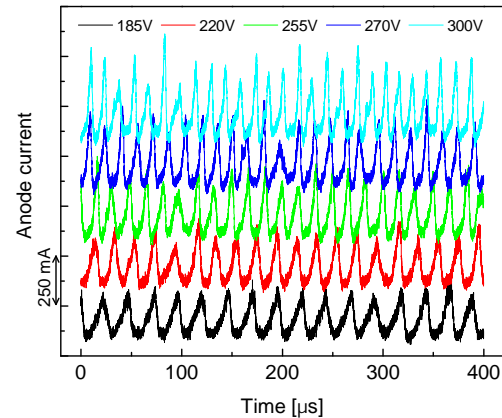


Figure 5. Oscillograms of discharge current. Xe flow rate is 0.17 mg/s.

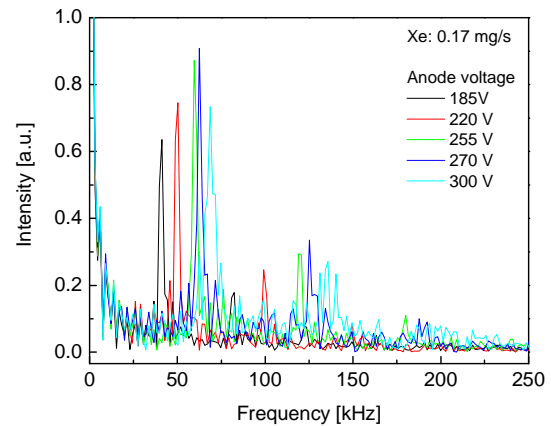


Figure 6. Low frequency spectral analysis of the discharge current (Xe 0.17 mg/s).

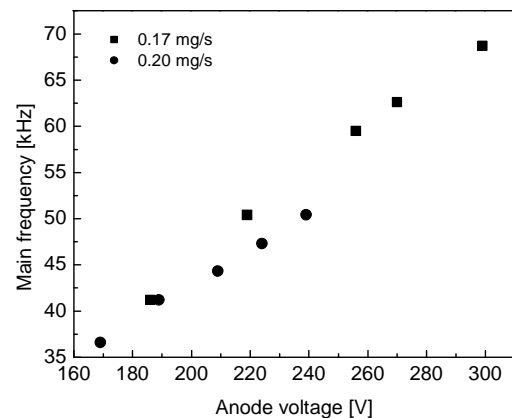


Figure 7. Mean fundamental “breathing mode” frequency as a function of the discharge voltage.

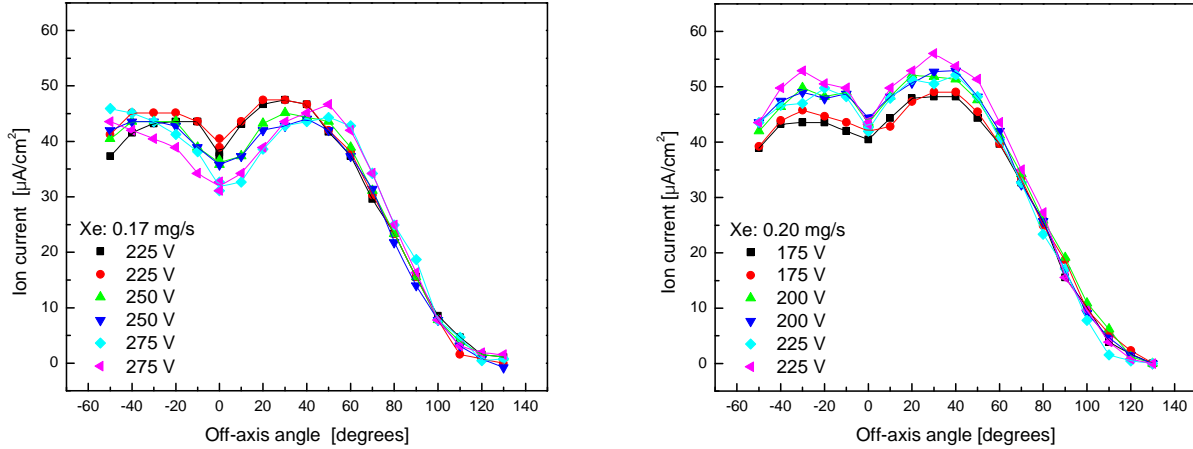


Figure 8. Ion current distributions measured at 22 cm downstream from the anode surface.

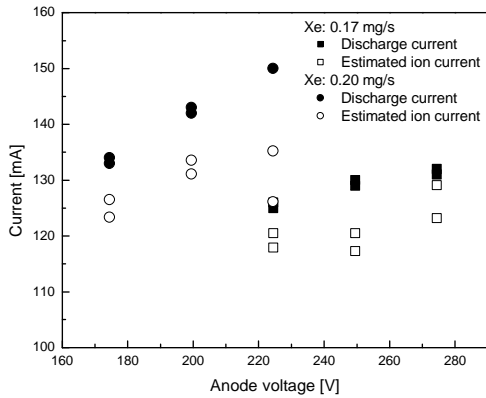


Figure 9. Discharge and ion currents as a function of the discharge voltage.

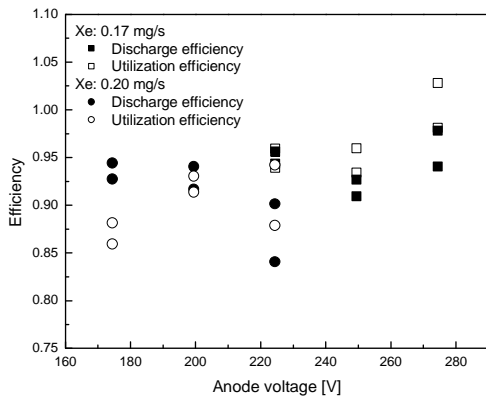


Figure 10. Discharge and Utilization efficiencies as a function of the discharge voltage. The effect of multiply charged ions is neglected.

is positioned on the negative angle side of the scale shown. A fairly large plume divergence was observed at all conditions. The peak density is located near 30-50° (i.e., off axis). In the lower (0.17 mg/s) flow case shown, higher voltage operation seems to shift this maximum towards greater angle – a tendency not seen in the 0.20 mg/s case. By spatial integration over the subtended solid angle of the spatial distribution, we can obtain the total ion current. The variation in the total ion current with voltage is shown in Fig. 9. Also shown in this figure are the discharge currents, for comparison. The ionization efficiencies, defined by the ratio of total ion current to discharge current, are estimated to be in the range of 85-95% as shown in Fig. 10. Of course, in estimating this efficiency, we have assumed that the fraction of doubly ionized xenon in the beam is negligible. The estimated uncertainty in the total ion current was ~ 20%.

C. Ion Energy Measurement

RPA measurements were performed with voltages referenced to the ground potential. Therefore, the analysis of the ion energy distribution requires a correction for the local plasma potential. The plasma potential at a downstream position of 7 cm from the thruster exit, where the RPA measurements were performed, was determined using an emissive probe, as described above. The plasma potential was found to be almost uniform (independent of angle) at this location, and measured to be 10 ± 2 V for every operation condition examined for the RPA analysis, although there appeared to be a slight decrease with increasing angle off of the centerline.

Examples of extracted ion energy distributions are shown in Fig. 11. The distributions shown have been corrected for a plasma potential of 10 V. The

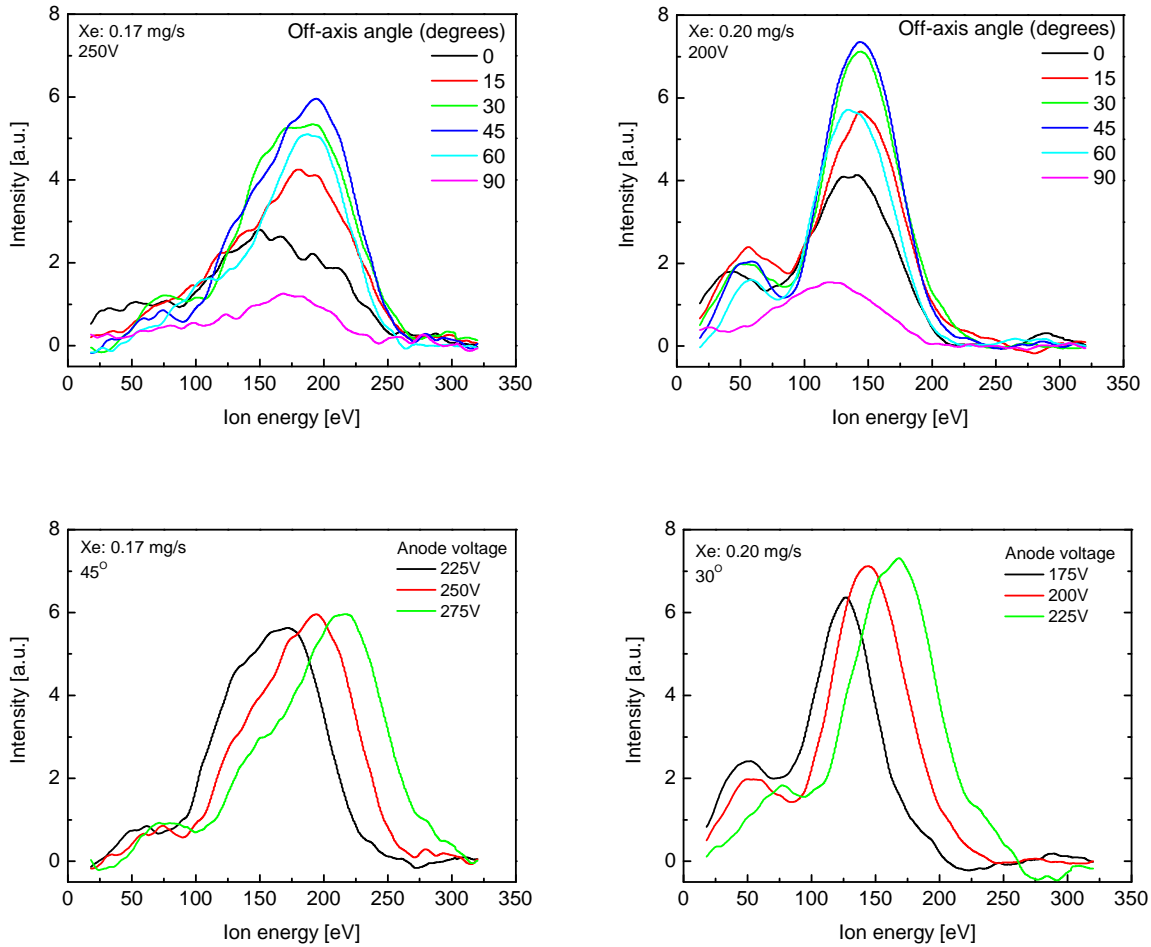


Figure 11. Examples of RPA measurements. Note: the energy is shifted from the observed value based on the ground potential by a plasma potential of 10V.

distribution is dominated by energetic ions peaked at a potential of approximately 50 eV lower than the discharge voltage. This 50 eV energy deficit seemed to be independent of the operating conditions. Most scans (more noticeably at higher mass flow rate) exhibit a low energy peak in the range of 50-80 eV. We believe that this peak may be due to charge exchange collisions between the ions in the beam and neutral xenon emitted by the hollow cathode. However, this low-energy peak may also reflect the presence of charge exchange collisions with non-ionized xenon exiting the anode, because it was not as strong for operating conditions at the lower anode flow rates.

The shape of the main peak is relatively broad in comparison to that seen in larger, higher power thrusters [8]. We attribute this to a relatively broad ionization zone, which is consistent with a relatively low frequency seen for the “breathing mode” instability. We suspect that this broad ionization zone might also be at the reason for the large beam divergence seen in the ion current measurements.

D. Thrust and Efficiency

Results of the thrusts measured directly using the thrust stand described above, are shown in Fig. 12. Although the thrust stand was configured with flexures that were more appropriate for a larger-size thruster (~ kW design), the measurements were performed despite a relatively large uncertainty of ~0.15mN, for comparison to indirect measurements based on the ion current and ion energy distribution. These indirect thrust measurements are also shown in Fig. 12. The thrust was found to be in the range of 0.6-1.6 mN for conditions of 0.20 mg/s and 110-225V, and 0.9-1.3 mN for 0.17 mg/s and a voltage of 200-275V. The direct thrust measurements are found to be in reasonable agreement with those estimated from plume parameters. However, it is noteworthy that the discharge

current monitored during the direct thrust measurements in the larger facility are slightly higher (by ~10%) than the discharge current observed during ion current and ion energy measurements in the smaller (higher backpressure) facility.

Figure 13 shows the resulting variation in thrust efficiency with discharge voltage. Thruster efficiency is seen to increase with increasing voltage, as expected, and is found to be in the range of approximately 10-15% for the voltage range examined here.

The variation in specific impulse with discharge voltage is shown in Fig. 14. The specific impulse is found to be in the range of 300-850s for conditions tested. This low specific impulse is attributed to the relatively low ion energy (due to the 50 eV deficit) in comparison to typical higher power thrusters. It seems that operation at higher specific impulse, and higher thrust efficiency will require high discharge voltage. However, thermal drifts and excessive heat transfer to the inner pole piece precluded operation at lower mass flow rates and higher discharge voltages, at this time. Future research will focus primarily on redesigning the discharge for improved thermal management of the inner pole piece, and a reconfiguration of the magnetic circuit for optimization of the magnetic field.

IV. Conclusions

The operation and performance characterization of a 4 mm diameter micro Hall thruster is presented. The characterization includes a measurement of plume ion current, ion energy, and thrust (direct and indirect). The thruster was operated in the 10-40W power range. A reasonable thrust level and high ionization efficiency has been confirmed. The thrust was found to be in the range of 0.6-1.6 mN. Thrust efficiency is estimated to be 10-15% with a specific impulse in the range of 300-850 s.

Despite of the successful operation of this thruster, it appears to have a relatively large beam divergence. This beam divergence, which we attribute to a broad ionization zone resulting from a less than optimum magnetic field distribution must be improved in future studies, for better performance. The presence of a broad ionization zone is consistent with a relatively low frequency seen for the “breathing mode” instability and the relatively broad ion energy distribution measured using an RPA.

Acknowledgments

This research was supported in part by the NSF/DOE Basic Plasma Initiative, and by the Air Force Office of Scientific Research. The authors would like to thank M. Bachand, C. Thomas, and E. Sommer for their technical assistance and helpful discussions. Partial support for T. Ito was provided by the JSPS Postdoctoral Fellowships for Research Abroad program.

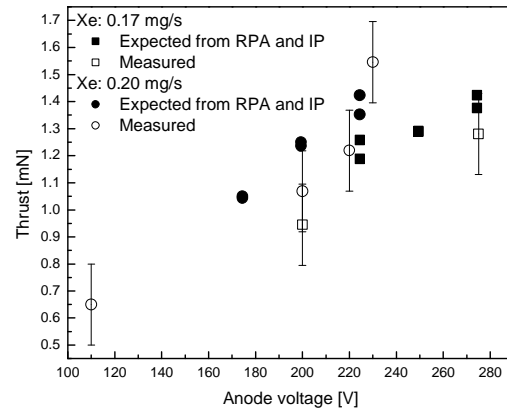


Figure 12. Thrust as a function of the discharge voltage.

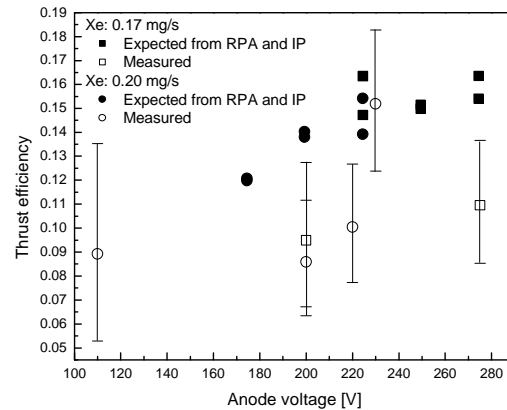


Figure 13. Thrust efficiency as a function of the discharge voltage.

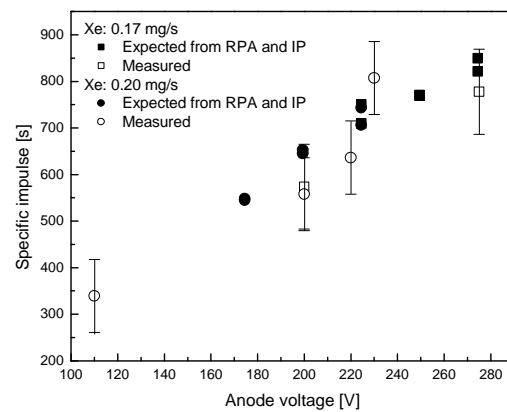


Figure 14. Specific impulse as a function of the discharge voltage.

References

- ¹Brown, C. O., and Pinsley, E. A., "Further Experimental Investigations of a Cesium Hall-Current Accelerator", *AIAA J.*, Vol. 3, 1965, pp. 853-859.
- ²Janes, G. S., and Lowder, R. S., "Anomalous Electron Diffusion and Ion Acceleration in a Low-Density Plasma", *Phys. Fluids.*, Vol. 9, 1966, pp. 1115-1123.
- ³Khayms, V., and Martinez-Sanchez, M., "Design of a Miniaturized Hall Thruster for Microsatellites", *32nd Joint Propulsion Conference*, Lake Buena Vista, FL, 1996, AIAA-96-3291.
- ⁴Schmidt, D. P., Meezan, N. B., Hargus, W. A. Jr., and Cappelli, M. A., "A Low-Power, Linear-Geometry Hall Plasma Source with an Open Electron-Drift", *Plasma Sources Sci. Technol.*, Vol. 9, 2000, pp. 68-76.
- ⁵Ito, T., Gascon, N., Crawford, W. S., and Cappelli M. A., "Ultra-Low Power Stationary Plasma Thruster", *The 29th International Electric Propulsion Conference, Princeton, Oct. 31- Nov. 4, 2005*.
- ⁶Meeker D. C., Finite Element Method Magnetics, Version 3.4.1, <http://femm.foster-miller.net>.
- ⁷Fife, J. M., "Hybrid-PIC Modeling and Electrostatic Probe Survey of Hall Thruster", *PhD Thesis, MIT, Cambridge, MA*, 1998.
- ⁸Hofer, R., Haas, J., Gallimore, A., "Ion Voltage Diagnostics in the Far-field Plume of a High-specific Impulse Hall Thruster", *39th Joint Propulsion Conference*, Huntsville, AL, 2003, AIAA-2003-4556.